IN REPLY REFER TO:

UNITED STATES
DEPARTMENT OF THE INTERIOR
GEOLOGICAL SURVEY
WASHINGTON 25, D. C.

AUG 18 1954

AEC-1103/4

Mr. Jesse C. Johnson, Director
Division of Raw Materials
U. S. Atomic Energy Commission
16th St. and Constitution Avenue, N.W.
Washington 25, D. C.

Dear Jesse:

Transmitted herewith are three copies of TEI-439, "Montroseite and paramontroseite," by Howard T. Evans, Jr., and Mary E. Mrose, June 1954.

We are asking Mr. Hosted to approve our plan to submit this report for publication in American Mineralogist.

Sincerely yours,

Andrew Bradley

for W. H. Bradley
Chief Geologist

Geology and Mineralogy

This document consists of 27 pages.
Series A.

UNITED STATES DEPARTMENT OF THE INTERIOR

GEOLOGICAL SURVEY

MONTROSEITE AND PARAMONTROSEITE*

By

Howard T. Evans, Jr., and Mary E. Mrose

June 1954

Trace Elements Investigations Report 439

This preliminary report is distributed without editorial and technical review for conformity with official standards and nomenclature. It is not for public inspection or quotation.

*This report concerns work done on behalf of the Division of Raw Materials of the U. S. Atomic Energy Commission.

USGS - TEI-439

GEOLOGY AND MINERALOGY

Distribution (Series A)	No. of copies
Argonne National Laboratory	1
Atomic Energy Commission, Washington	2
Battelle Memorial Institute, Columbus	1
Carbide and Carbon Chemicals Company, Y-12 Area	1
Division of Raw Materials, Albuquerque	1
Division of Raw Materials, Butte	1
Division of Raw Materials, Denver	1
Division of Raw Materials, Douglas	1
Division of Raw Materials, Hot Springs	1
Division of Raw Materials, Ishpeming	1
Division of Raw Materials, Phoenix	1
Division of Raw Materials, Richfield	1
Division of Raw Materials, Salt Lake City	1
Division of Raw Materials, Washington	3
Dow Chemical Company, Pittsburg	1
Exploration Division, Grand Junction Operations Office	1
Grand Junction Operations Office	1
National Lead Company, Winchester	1
Technical Information Service, Oak Ridge	6
Tennessee Valley Authority, Wilson Dam	1
U. S. Geological Survey:	
Alaskan Geology Branch, Washington	1
Fuels Branch, Washington	1
Geochemistry and Petrology Branch, Washington	21
Geophysics Branch, Washington	1
Mineral Deposits Branch, Washington	1
E. H. Bailey, Menlo Park	1
A. L. Brokaw, Grand Junction	1
K. L. Buck, Denver	1
J. R. Cooper, Denver	1
N. M. Denson, Denver	1
C. E. Dutton, Madison	1
W. L. Emerick, Plant City	1
L. S. Gardner, Albuquerque	1
M. R. Klepper, Washington	1
A. H. Koschmann, Denver	1
R. A. Laurence, Knoxville	1
D. M. Lemmon, Washington	1
J. D. Love, Laramie	1
V. E. McKelvey, Menlo Park	1
Q. D. Singewald, Beltsville	1
J. F. Smith, Jr., Denver	1
A. O. Taylor, Salt Lake City	1
A. E. Weissenborn, Spokane	1
TEPCO, Denver	2
TEPCO, RPS, Washington	2
(Including master)	
	75

CONTENTS

ILLUSTRATIONS

TABLES

MONTROSEITE AND PARAMONTROSEITE

By Howard T. Evans, Jr., and Mary E. Mrose

ABSTRACT

Montroseite (V,Fe)O(OH), has been shown by Evans and Block to have a structure analogous to that of diaspore, AlO(OH). Altered crystals of montroseite give multiple X-ray patterns, showing one sharp orthorhombic lattice corresponding to the host crystal, and two diffuse lattices of similar symmetry and dimensions in parallel orientation. The more prominent of the diffuse phases is interpreted as a metastable form of VO_2, resulting from the oxidation of the host crystal, and is given the name "paramontroseite". Paramontroseite has $\underline{a}$ = 4.89, $\underline{b}$ = 9.39, $\underline{c}$ = 2.93 A, space group Pbnm. Complete refinement of the structure of both montroseite and paramontroseite has been carried out by electron density synthesis and least squares analysis. The outstanding difference between the two structures lies in the length of the oxygen-oxygen distance corresponding to the hydrogen bond in montroseite. This length increases from 2.63 to 3.87 A in going from montroseite to paramontroseite, indicating the loss of hydrogen during the alteration. The concept of an alteration process involving a migration of ions and electrons through an unbroken oxygen framework is thus directly supported by the crystal structure analyses, and also by other X-ray diffraction and chemical information. The postulated alteration mechanism is illustrated by certain other examples, notably the alteration of lepidocrocite and magnetite to maghemite, and goethite to hematite.

INTRODUCTION

In a recent communication by Weeks, Cisney, and Sherwood (1953), the discovery, properties, and mode of occurrence of a new mineral from the Colorado Plateaus region, montroseite, were described. The material forms submetallic, greyish-black bladed crystalline masses. In cavities it forms small lathlike crystals with a perfect (010) cleavage. The density was measured on one sample as 4.00. The essential constitution of montroseite was demonstrated, by means of a detailed crystal structure analysis by Evans and Block (1953), to consist of a vanadium oxide hydrate with the basic formula VO(OH), analogous to diaspore, AlO(OH). These authors pointed out that diffraction patterns obtained from apparently single crystals of montroseite are multiple, showing the presence of at least three phases. The multiple diffraction patterns show three orthorhombic lattices in parallel position, with slightly varying lattice constants, one characterized by sharp diffraction spots, the other two by diffuse spots. Figure 1 shows part of a Buerger precession photograph of the (0k$\underline{l}$) plane on which the sharp and the "diffuse B" lattices are clearly visible. The data given for these lattices by Evans and Block are reproduced in table 1.

It was tentatively suggested by Evans and Block that the sharp lattice (for which the structure analysis was carried out) represents the original host phase which subsequently alters by atmospheric action to give rise to the diffuse phases. New information has now been obtained concerning this alteration process as a result of a complete structure analysis of the "diffuse B" phase, which is described in this paper. The evidence is sufficient to define the chemical nature of the "diffuse B" phase, and

establish it as a new mineral species. Therefore, because of the paramorphic relationship that it has to the host mineral montroseite, as described more fully below, we propose for the "diffuse B" phase the name paramontroseite.

As a result of the study described herein, it has been possible to show by the direct methods of X-ray diffraction and crystal structure analysis that the naturally occurring crystals of the mineral are actually in part or wholly pseudomorphs of the new mineral, paramontroseite, after the original montroseite. The anomalous and variable results of chemical analysis are fully explained and, further, the mechanism of alteration by oxidation and dehydrogenation is revealed.

SOURCE OF THE DATA

Crystals of montroseite from the Bitter Creek mine, Paradox Valley, Colo., were used for the structure investigations. The first crystal to be photographed showed all three phases present--the montroseite and paramontroseite lattices being about equally intense, the "diffuse A" lattice much weaker. The spots were streaked in a manner to indicate a distortion of the crystal around the c axis of 10 degrees or more, a habit which is apparently characteristic of montroseite crystals. The intensity data for montroseite were measured by visual estimates of 99 observed (hk0) reflections from this crystal registered on a Weissenberg pattern using MoKα radiation, as described by Evans and Block (1953). A second altered crystal of montroseite gave a nearly pure paramontroseite pattern, with only slight traces of the strongest reflections of the montroseite lattice still discernible. This crystal was used to measure 34 observed (hk0) reflections by visual estimates made on a Weissenberg pattern made with CuKα radiation. No corrections were made for absorption.

Despite the distortions inherent in the crystals, the data for montroseite give excellent agreement with those calculated for the proposed structure, but those for the diffuse phase are of very poor quality. Both sets of data have been treated by the method of least squares as described below, in order to ensure the determination of the most likely structures and at the same time derive the standard errors appropriate to each.

DETERMINATION OF THE CRYSTAL STRUCTURE OF PARAMONTROSEITE

The distribution of intensity among the (hk0) reflections for paramontroseite is quite similar to, though differing markedly in detail from, that of montroseite as reported by Evans and Block (1953). (See table 3, p. 19.) On the assumption that the paramontroseite structure is similar to that of montroseite, the Patterson projection along [001] was partly computed in order to locate the V-V interatomic distance vectors. Peaks were found near the expected positions, and from them vanadium parameters were obtained from which the first set of structure factors were calculated (oxygen atoms omitted). These structure factors for vanadium yielded probable Fourier phases for the 34 observed (hk0) terms, permitting the synthesis of the electron density projected along the c axis. Peaks corresponding to oxygen atoms were clearly apparent in this map, and the second set of calculated structure factors included all atoms in the cell, with coordinates read from the electron density map. The usual electron density synthesis-structure factor cycle was repeated twice more, until the map coordinates were consistent with all the phases. The final electron density projection is shown in figure 2b. Figure 2a shows the corresponding electron density projection of montroseite from Evans and Block (1953) for comparison. The atom coordinates as measured from these maps by

parabolic interpolation are given in table 2.

REFINEMENT OF THE MONTROSEITE AND PARAMONTROSEITE STRUCTURES BY THE METHOD OF LEAST SQUARES

Because of the distortions in the electron density maps caused by inaccuracies in the intensity measurements and series termination effects, the method of least squares was used to derive the most likely structure consistent with the original data. The method was applied in a straightforward manner as described in several other places. (See, for example, Shoemaker, Donahue, Schomaker, and Corey, 1950.) The analysis is based on the structure factor function

$$\underline{F}_{calc} = e^{-\underline{B}\underline{s}^2} \sum_j \underline{f}_j \cos 2\pi(\underline{h}\underline{x}_j + \underline{k}\underline{y}_j + \underline{\ell}\underline{z}_j)$$

where $\underline{B}$ is the temperature coefficient, $\underline{s} = (\sin \theta)/\lambda$, $\underline{f}_j$ is the scattering factor for the atom $\underline{j}$, and $\underline{x}_j$, $\underline{y}_j$ are $\underline{z}_j$ are coordinates of each atom $\underline{j}$. The seven parameters to be determined are $\underline{x}(V)$, $\underline{y}(V)$, $\underline{x}(O_I)$, $\underline{y}(O_I)$, $\underline{x}(O_{II})$, $\underline{y}(O_{II})$, and $\underline{B}$. As all atoms are well separated in the $\underline{c}$ axis projection, all nondiagonal terms in the normal equations were neglected. The only matter of judgment concerns the manner in which the observations should be weighted in deriving the normal equations. Using these considerations, the normal equations reduce to a series of independent linear equations in terms of correction terms $\Delta\underline{x}$, to be applied to each of the structure parameters:

$$\left[\sum \underline{w}\left(\frac{\partial \underline{F}}{\partial \underline{x}}\right)^2\right]\Delta\underline{x} = \sum \underline{w}\left(\frac{\partial \underline{F}}{\partial \underline{x}}\Delta\underline{F}\right)$$

where $\Delta\underline{F} = (\underline{F}_{obs} - \underline{F}_{calc})$, $\underline{x}$ is the structure parameter $\underline{x}(V)$, $\underline{y}(V)$, $\underline{x}(O_I)$, etc., and $\sqrt{\underline{w}}$ is the weight given to each observation. If intensity as measured is a logarithmic function of film density in which errors of

estimate by the eye are assumed to be distributed normally, it can easily be shown that the appropriate weighting factor is

$$\sqrt{w} = 1/E$$

Although experience seems to show that such an assumption is somewhere near the truth, the point is controversial, and we have carried out analyses with both

$$\sqrt{w} = \frac{1}{E} \quad \text{(weighted) and}$$

$$\sqrt{w} = 1 \quad \text{(unweighted).}$$

We accept the structures derived from the weighted analysis as the best, but it is observed that the difference between the weighted and unweighted results is generally less than the calculated standard errors. The standard error of E is

$$\epsilon_E = \sqrt{\frac{\sum w(\Delta E)^2}{n-p}}$$

where n is the number of observations (99 for montroseite, 34 for para-montroseite) and p the number of parameters (7, including the temperature factor, B). The standard error of x, ϵ_x, is given by

$$\epsilon_x^2 = \frac{\epsilon_E^2}{\sum w\left(\frac{\partial E}{\partial x}\right)^2}$$

The ΔE values were obtained by scaling E_{obs} by multiplying by

$$k = \frac{\sum |E_{calc}| \cdot |E_{obs}|}{\sum |E_{obs}|^2}$$

for unweighted calculations, and

$$k = \frac{1}{n} \sum \frac{|E_{calc}|}{|E_{obs}|}$$

for weighted calculations. Actually, the value of k is not very critical, except in the case of the weighted calculations of ΔB for the temperature corrections, where it was found necessary to take account of the cross-

product terms between ΔB and Δk.

The results of all calculations for both montroseite and paramontroseite are given in table 2. The final parameters for montroseite and paramontroseite used to determine bond lengths in the following section are those listed under the columns labeled "weighted" in this table.

The reliability factor

$$R = \frac{\Sigma |\Delta F|}{\Sigma |F_{obs}|}$$

obtained with

$$k = \frac{\Sigma |F_{calc}|}{\Sigma |F_{obs}|}$$

has a value $R = 0.113$ for 99 observed reflections for montroseite, and $R = 0.24$ for 34 non-zero reflections for paramontroseite. Observed and calculated structure factors for montroseite and paramontroseite are listed in table 3*.

STRUCTURAL FEATURES OF MONTROSEITE AND PARAMONTROSEITE

The interatomic distances defined in figure 3 are tabulated for both structures in table 4. The standard errors of the lengths shown are derived from those associated with the parameters given in table 2. It is found that the errors in location of most atoms are practically isotropic, and have magnitudes shown in table 5. Errors on interatomic distances r between atoms A and B are given by:

$$\epsilon_r^2 = \epsilon_A^2 + \epsilon_B^2 + (\epsilon'_L r)^2$$

where ϵ'_L is the error of lattice measurement in percent.

---

*Because of an error made in the calculations, the values of F_{calc} for reflections with k odd in table 2 of the paper by Evans and Block (1953) are incorrect. This error does not affect any other data given in that paper, except that $R = 0.11$ instead of 0.21.

It is clear that the essential principles of coordination and vanadium-oxygen bonding are the same in both montroseite and paramontroseite. The main difference between these structures, as shown by the c axis elevations shown in figure 4, lies in the fact that the zig-zag octahedron chains have rotated some 28 degrees around the c axis direction in passing from one to the other. This process has been accompanied by two important changes in the structure:

(1) First and most important, the interoxygen distance, H, is short (2.63 A) in montroseite, but very long (3.87 A) in paramontroseite. The former value is very reasonable for a hydrogen bond, as suggested by Evans and Block (1953), but the latter is far too large for such a bond. As there is no other logical place for hydrogen in the structure, the conclusion must be drawn that hydrogen is absent in paramontroseite.

(2) Second, the vanadium-oxygen distances are slightly, but probably significantly shorter in paramontroseite than in montroseite. The change is close to that which would be expected when one electron pair is added to the montrosiete vanadium bond coordination system; i.e., when vanadium is oxidized from +3 to +4 through the loss of hydrogen.

SOLID STATE ALTERATION OF MONTROSEITE

In light of the known facts, the history of the mineral montroseite may be outlined as follows:

(a) The mineral montroseite, VO(OH), (with some Fe usually replacing V), is deposited in crystalline masses, by an unknown process, in the sandstone matrix.

(b) The crystallized montroseite is oxidized by oxygen in the atmosphere or in ground water to paramontroseite, at temperatures below 50° C, according to the reaction:

$$\underset{\text{(Montroseite)}}{2VO(OH)} + \tfrac{1}{2}O_2 \longrightarrow \underset{\text{(Paramontroseite)}}{2VO_2} + H_2O$$

(c) The oxidation process is accomplished by a migration of the hydrogen atoms through the montroseite crystal structure to the crystal surface where they combine with oxygen. The close-packed oxygen framework is slightly shifted in this process but is not broken down. The process may pass through an intermediate stage involving the "diffuse A" phase.

(d) The end product of this solid state alteration process, paramontroseite, is itself unstable, and is subsequently destroyed by weathering action and replaced by the corvusite type of minerals.

These conclusions are drawn from the following established facts:

1. The montroseite phase gives rise to a sharp diffraction pattern, suggesting normal crystal growth of a primary phase.

2. The paramontroseite diffraction pattern is diffuse, suggesting that this phase occurs as alteration nucleii finely disseminated through the host crystal, as would be expected to result from the postulated diffusion of hydrogen atoms.

3. The structure of montroseite and paramontroseite, especially the nearly hexagonal close-packed oxygen framework, is the same.

4. The crystal lattices of montroseite and paramontroseite are in parallel position.

5. The average temperature vibration amplitude for montroseite ($= \sqrt{B/8\pi^2}$) is 0.21 A indicating a firmly bound, stable structure, whereas the average amplitude of paramontroseite is 0.53 A indicating a much less stable structure. The difference in temperature vibration accounts for the much larger and more diffuse appearance of the vanadium atoms in the electron density map of paramontroseite as compared with montroseite (fig. 2).

6. The hydrogen bond length of montroseite has greatly increased in paramontroseite, indicating loss of hydrogen.

7. The vanadium-oxygen distances in montroseite are longer than in paramontroseite, indicating oxidation of the vanadium.

8. The powder patterns of montroseite can be indexed on a lattice which conforms most closely with the paramontroseite lattice (Weeks, Cisney, and Sherwood, 1953). Actually, calculated and observed interplanar spacings show fair agreement, using lattice parameters intermediate between the "diffuse A" and "B" lattices.

9. Chemical analyses (Weeks, Cisney, and Sherwood, 1953) show extensive, in some cases nearly complete, replacement of V_2O_3 by V_2O_4. Also, the water content is decreased consistently with the oxidation of VO(OH) to VO_2.

It has been mentioned that there is evidence for a third phase present in montroseite crystals, referred to as the "diffuse A" phase. The true nature of the "diffuse A" phase is unknown. Its relation to the montroseite and paramontroseite suggests that it may represent an intermediate step in the alteration of one into the other. If this is the case, the "diffuse A" phase may be $V_2O_3(OH)$, having the space group $\underline{Pb2_1m}$ (C^2_{2v}) or $\underline{P2_1nm}$ (C^7_{2v}), with 2 formula units per cell. This non-centrosymmetric phase would correspond to the montroseite structure with half the hydrogen atoms removed. Alternatively, the "diffuse A" phase may represent some sort of separated Fe-rich phase, but its constants are not the same as those of goethite.

OTHER EXAMPLES OF SOLID STATE ALTERATION PHENOMENA

It is well known that the cubic polymorph of Fe_2O_3 can be prepared by warming magnetite (Fe_3O_4) in a stream of oxygen at low temperatures ($< 250^{\circ}C$). At higher temperatures the cubic γ-Fe_2O_3 is converted to the rhombohedral

α-Fe_2O_3. It is understood that the oxidation occurs without disturbing the cubic close-packed oxygen framework of the spinel structure of magnetite. The oxygen lattice grows at the crystal surface, and the Fe atoms diffuse outward until the spinel-type unit cell contents $Fe_{24}O_{32}$ is reduced to $Fe_{21\frac{1}{3}}O_{32}$. Evidently, γ-Fe_2O_3 is wholly metastable, and can only exist as a result of a low temperature chemical change in the solid state from a stable phase.

This phenomenon probably accounts for the observation by Newhouse (1929), that magnetite crystals from Magnet Cove, Ark., are coated with an oriented over-growth of maghemite (γ-Fe_2O_3). Maghemite also is known (Sosman and Posnjak, 1925) as an alteration product of lepidocrocite, FeO(OH), which has a structure based on a cubic close-packed oxygen lattice, whereas hematite (α-Fe_2O_3) is a common alteration product of goethite, which has the diaspore structure like montroseite. These two examples do not involve oxidation but the alteration process is probably similar to that of montroseite and magnetite.

Artificial vanadium dioxide does not have the paramontroseite structure, but rather a distorted rutile structure (Andersson, 1953). Paramontroseite is probably also metastable like maghemite, and can only exist through solid state alteration from the stable montroseite at low temperatures. These minerals are most nearly analogous to groutite (MnO(OH)) and ramsdellite (MnO_2), both having the diaspore structure, but unfortunately there has been no study yet of the paragenetic relationships of the two manganese minerals which would enable us to compare our conclusions regarding the vanadium minerals.

SUMMARY

The crystal structures of montroseite, VO(OH), and paramontroseite, VO_2, have been refined by the method of least squares. Both are based on the diaspore structure type. Montroseite crystals give multiple X-ray diffraction patterns, a sharp pattern which has yielded the data for montroseite, and a diffuse pattern which gave the data for paramontroseite. An outstanding difference between the two phases revealed by the structure analysis is that a hydrogen bond which is present in montroseite is absent in paramontroseite. Thus, the chemical nature of the two phases is confirmed and paramontroseite is established as a new species. In addition, the paramorphic relationship between the two is well explained.

Crystal structure data, lattice studies, certain diffraction phenomena, and chemical data have all led to the conclusion that montroseite alters to paramontroseite through weathering action, by means of a solid state reaction at low temperature. This process involves the migration of hydrogen atoms through an unchanged hexagonal close-packed oxygen framework. Paramontroseite is evidently a metastable phase. The alteration of montroseite to paramontroseite is apparently analogous with that of magnetite to maghemite, lepidocrocite to maghemite, and goethite to hematite.

REFERENCES

Andersson, G., 1953, X-ray studies on vanadium oxides: Research, v. 6, p. 455-465.

Evans, H. T., Jr., and Block, S., 1953, The crystal structure of montroseite, a vanadium member of the diaspore group: Am. Mineralogist, v. 38, p. 1242-1250.

Newhouse, W. H., 1929, The identity and genesis of loadstone magnetite: Econ. Geology, v. 24, p. 62-67.

Shoemaker, D. P., Donahue, J., Schomaker, V., and Corey, R. B., 1950, The crystal structure of L_s-threonine, Am. Chem. Soc. Jour., v. 72, p. 2328-2349.

Sosman, R. B., and Posnjak, E., 1925, Ferromagnetic ferric oxide, artificial and natural: Washington Acad. Sci. Jour., v. 15, p. 329-344.

Weeks, A. D., Cisney, E., and Sherwood, A. M., 1953, Montroseite, a new vanadium oxide from the Colorado Plateaus: Am. Mineralogist, v. 38, p. 1235-1241.

Table 1.--Lattice data for montroseite phases.

	Montroseite	"Diffuse A"	Paramontroseite "Diffuse B"
Formula	VO(OH)	$V_2O_3(OH)$(?)	VO_2
a (A)	4.54	4.80	4.89
b (A)	9.97	9.63	9.39
c (A)	3.03	2.93	2.93
V (A^3)	136.9	135.4	134.4
d (calc. for 8% FeO)	4.11	4.15	4.18
Z (formula units)	4	2	4
Space group	Pbnm (D_{2h}^{16})	$Pb2_1m$ (?) (C_{2v}^{2})	Pbnm (D_{2h}^{16})

Table 2.--Least squares-determined parameters and standard errors for montroseite and paramontroseite.

Par.	Montroseite					Paramontroseite				
	Elec. dens.	Unweighted Parameter	ϵ	Weighted* Parameter	ϵ	Elec. dens.	Unweighted Parameter	ϵ	Weighted Parameter	ϵ
x_V	-0.051	-0.0511	0.00086	-0.0517	0.00054	0.094	0.091	0.0048	0.088	0.0034
y_V	0.145	0.1457	0.00035	0.1455	0.00019	0.145	0.144	0.0027	0.143	0.0015
x_{OI}	0.297	0.300	0.0034	0.301	0.0021	0.127	0.091	0.0174	0.106	0.0181
y_{OI}	-0.197	-0.201	0.0016	-0.197	0.0011	-0.243	-0.254	0.0099	-0.235	0.0054
x_{OII}	-0.197	-0.199	0.0030	-0.198	0.0021	-0.232	-0.231	0.0197	-0.227	0.0157
y_{OII}	-0.051	-0.053	0.0016	-0.054	0.0011	-0.012	-0.018	0.0097	-0.013	0.0039
B		0.49	0.033	0.32	0.041		2.12	0.398	2.42	0.867

*The reflection (970) has been omitted from this analysis because of its disproportionately high weighting factor.

Table 3.--Observed and calculated structure factors for montroseite and paramontroseite.

	Montroseite		Paramontroseite	
hkl	F_{obs}	F_{calc}	F_{obs}	F_{calc}
020	18.9	-19.5		13
040	42.2	-46.0	8	-14
060	32.3	36.6	14	27
080	5.1	5.6	17	26
0,10,0	27.4	-34.8	11	-17
0,12,0	9.6	-10.7		
0,14,0	28.6	23.6		
0,16,0		- 4.3		
0,18,0	12.6	-13.6		
0,20,0	14.6	18.7		
110	56.2	51.7	34	43
120	33.9	22.2	46	-40
130	53.9	-48.9	46	-48
140	52.2	-44.6	5	7
150	14.0	-13.2		- 1
160	9.6	-11.9		13
170	42.2	43.1	26	26
180		1.9	16	-17
190	11.8	-15.7		- 3
1,10,0		2.6		- 4
1,11,0	28.0	-29.0		-12
1,12,0		- 1.0		
1,13,0	17.7	19.7		
1,14,0		1.3		
1,15,0	11.4	8.4		
1,16,0	11.8	13.2		
1,17,0	17.3	-15.5		
1,18,0		- 2.3		
1,19,0		1.7		
1,20,0		- 4.2		
1,21,0	13.8	12.7		
200	19.3	17.7	16	3
210	14.4	19.0	15	-24
220	11.2	-11.7	32	-21
230	12.6	9.8	32	-34
240	52.6	-42.8	19	-27
250	38.4	-35.8	35	44
260	24.2	23.8		0
270	5.9	- 6.2	7	- 9
280	25.6	28.2		2
290	20.6	24.5	10	-14
2,10,0	21.0	-25.5	7	- 8

Table 3.--Observed and calculated structure factors for montroseite and paramontroseite--Continued.

hkl	Montroseite F_{obs}	Montroseite F_{calc}	Paramontroseite F_{obs}	Paramontroseite F_{calc}
2,11,0	8.7	-11.8		
2,12,0		5.0		
2,13,0	6.3	- 6.2		
2,14,0	17.4	18.8		
2,15,0	13.6	14.7		
2,16,0	10.8	-10.3		
2,17,0		2.6		
2,18,0	11.6	- 9.6		
2,19,0		- 6.1		
2,20,0				
310	11.0	10.1	8	- 9
320	42.2	37.0	48	-35
330	37.6	-37.0		3
340	5.1	- 5.3	7	17
350		4.0		- 3
360	20.6	-24.4	11	22
370	20.2	21.0		- 4
380	26.5	28.7	10	-15
390		0		- 1
3,10,0	7.4	8.0		
3,11,0	8.7	- 6.8		
3,12,0	22.3	-25.2		
3,13,0		8.7		
3,14,0		3.7		
3,15,0		8.2		
3,16,0	11.4	9.5		
3,17,0	14.6	-13.3		
3,18,0		- 8.3		
3,19,0		- 2.9		
400	17.0	17.0	22	-24
410	39.4	40.7	16	-14
420		- 3.7	17	16
430	17.0	17.0		-10
440	8.1	- 8.0	15	10
450	23.4	-27.4	16	18
460	7.5	7.1		- 3
470	9.1	12.3		- 2
480		1.4		- 6
490	22.2	21.6	7	- 6
4,10,0		- 6.6		
4,11,0	10.8	-12.2		
4,12,0		- 2.6		
4,13,0	22.3	-19.0		

Table 3.--Observed and calculated structure factors for montroseite and paramontroseite--Continued.

	Montroseite		Paramontroseite	
hkl	F_{obs}	F_{calc}	F_{obs}	F_{calc}
4,14,0		5.2		
4,15,0		10.0		
4,16,0		- 0.8		
4,17,0		3.3		
4,18,0		- 3.7		
4,19,0	14.8	-17.1		
510		3.7		-10
520	30.7	32.1	7	- 4
530	10.8	10.3	19	19
540	13.8	-15.0		1
550	7.4	- 6.2		15
560	21.0	-20.1		1
570		0	6	-10
580	22.7	21.9		
590		- 5.1		
5,10,0	10.4	7.0		
5,11,0		- 6.1		
5,12,0	18.9	-20.2		
5,13,0		1.6		
5,14,0		2.6		
5,15,0		- 3.7		
5,16,0	17.4	13.4		
600		- 6.0	15	-14
610	14.4	13.4		2
620		3.3		3
630	6.5	8.7		
640		8.5		
650	28.4	-27.0		
660		- 5.8		
670		- 4.6		
680		- 6.6		
690	22.0	21.7		
6,10,0		5.4		
6,11,0	10.2	-11.9		
6,12,0		- 1.5		
6,13,0		- 5.4		
6,14,0		- 5.3		
6,15,0	12.8	16.4		
710	10.6	-10.3		
720	17.1	16.0		
730	8.1	6.7		
740	12.6	-13.0		

Table 3.--Observed and calculated structure factors for montroseite and paramontroseite--Continued.

	Montroseite		Paramontroseite	
hkl	F_{obs}	F_{calc}	F_{obs}	F_{calc}
750		6.1		
760	12.0	-12.8		
770	12.8	-12.6		
780	10.8	9.8		
790		7.1		
7,10,0		3.7		
7,11,0	11.0	12.4		
7,12,0		- 8.3		
800	20.8	-21.7		
810	9.5	11.1		
820		2.9		
830		3.8		
840	12.6	10.7		
850		- 7.3		
860	11.0	- 9.3		
870		4.1		
880		- 1.4		
890		5.1		
8,10,0	11.8	11.9		
910	10.0	- 8.5		
920		3.5		
930	15.5	14.3		
940		5.0		
950		0.5		
960		- 2.1		
970	5.7	11.8		
10,0,0	9.5	5.7		
10,1,0		- 0.9		
10,2,0		2.9		
10,3,0		0.5		
10,4,0	11.6	11.9		
10,5,0		1.3		
10,6,0	8.5	- 7.6		
10,7,0		0		
10,8,0	10.0	-10.4		
11,1,0		- 4.7		
11,2,0		- 3.6		
11,3,0	9.1	9.5		

Table 5.--Standard errors of atomic positions in montroseite and paramontroseite.

	Montroseite	Paramontroseite
ϵ_v	0.0037 A	0.015 A
ϵ_o	0.015 A	0.070 A
ϵ'_L	0.3 percent	0.5 percent

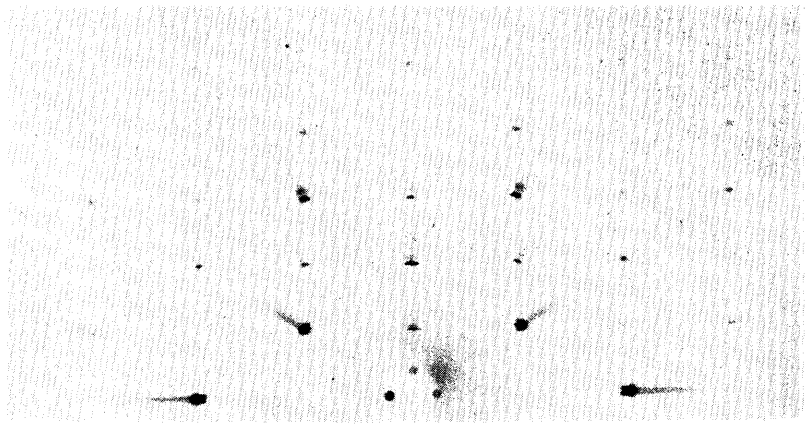

Figure 1.--Buerger precession photograph of the (0k$\underline{\ell}$) net plane of a montroseite crystal showing sharp and diffuse spots.

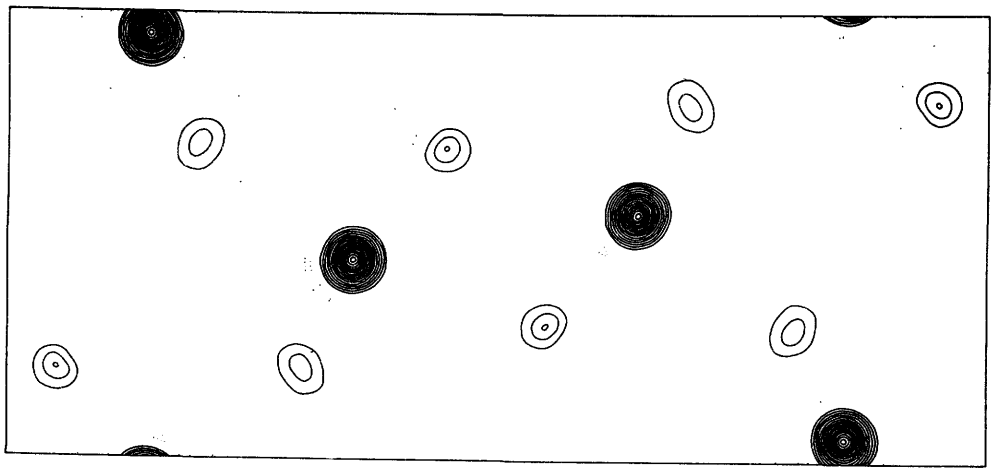

(a)

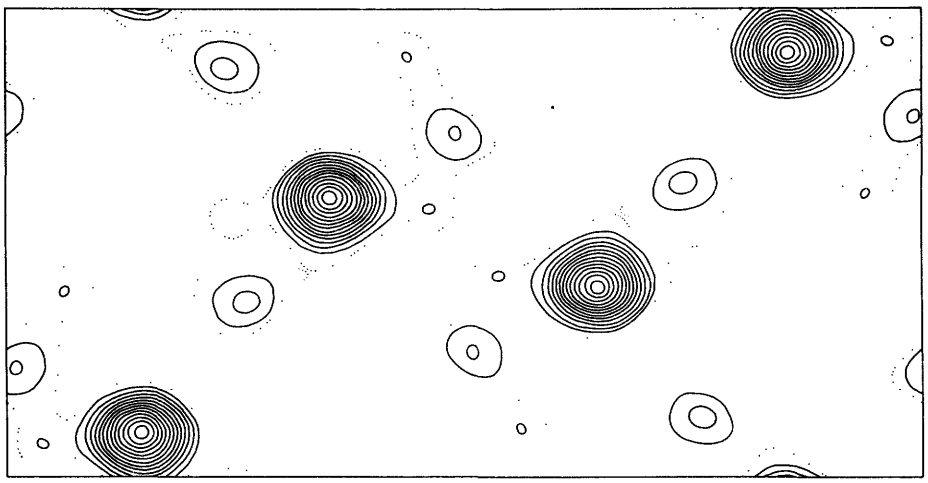

(b)

Figure 2.--Electron density projections along the c axis of (a) montroseite and (b) paramontroseite. Dotted contour represents 2 electrons per A^2; other contours at intervals of $2e/A^2$.

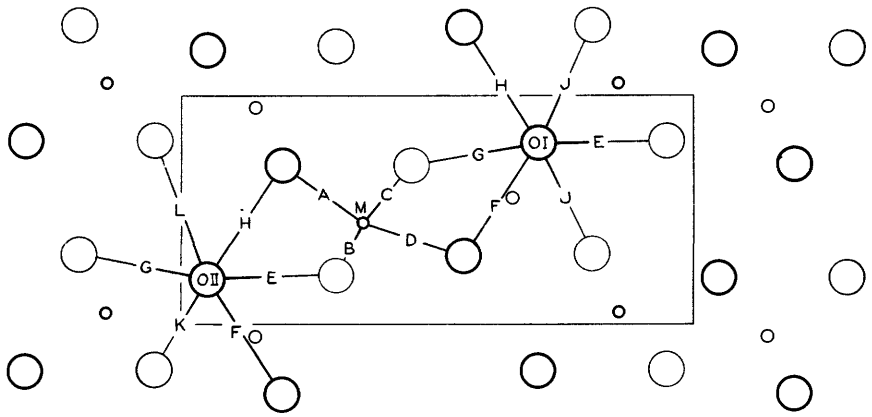

Figure 3.--Interatomic distance vectors in montroseite and paramontroseite. (See table 4.)

Table 4.--Interatomic distances in montroseite and paramontroseite.

Atoms	Vector	Montroseite (A)		Paramontroseite (A)	
$V-O_I$	A	1.94	± 0.017	1.88	± 0.07
	B(2)	1.96	± 0.017	1.91	± 0.07
$V-O_{II}$	C(2)	2.10	± 0.017	2.00	± 0.07
	D	2.10	± 0.017	2.13	± 0.07
O_I-O_{II}	E(2)	2.91	± 0.02	2.88	± 0.10
	F	2.68	± 0.02	2.65	± 0.10
	G(2)	2.96	± 0.02	2.79	± 0.10
	H	2.63	± 0.02	3.87	± 0.10
O_I-O_I	J(4)	2.93	± 0.02	2.86	± 0.10
	c-axis (2)	3.03	± 0.01	2.93	± 0.02
$O_{II}-O_{II}$	K(2)	2.59	± 0.02	2.65	± 0.10
	L(2)	3.31	± 0.02	3.04	± 0.10
V-V		3.306	± 0.011	3.16	± 0.03

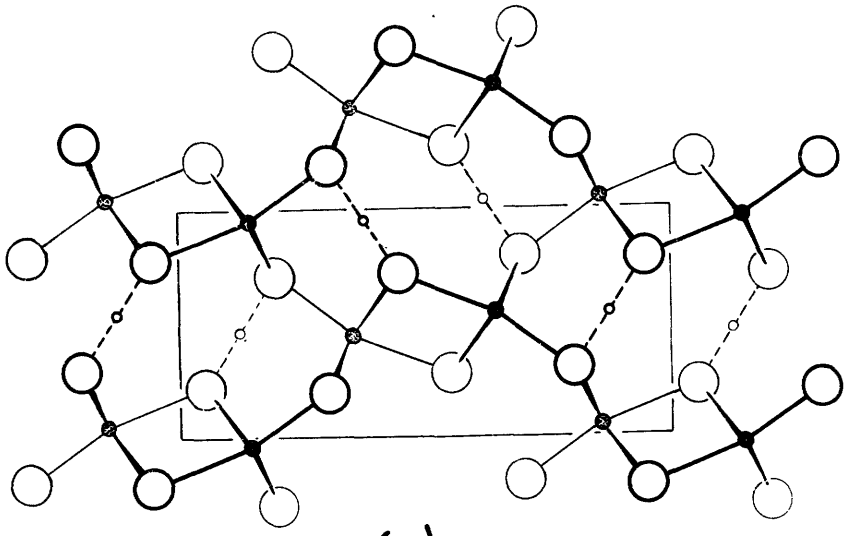

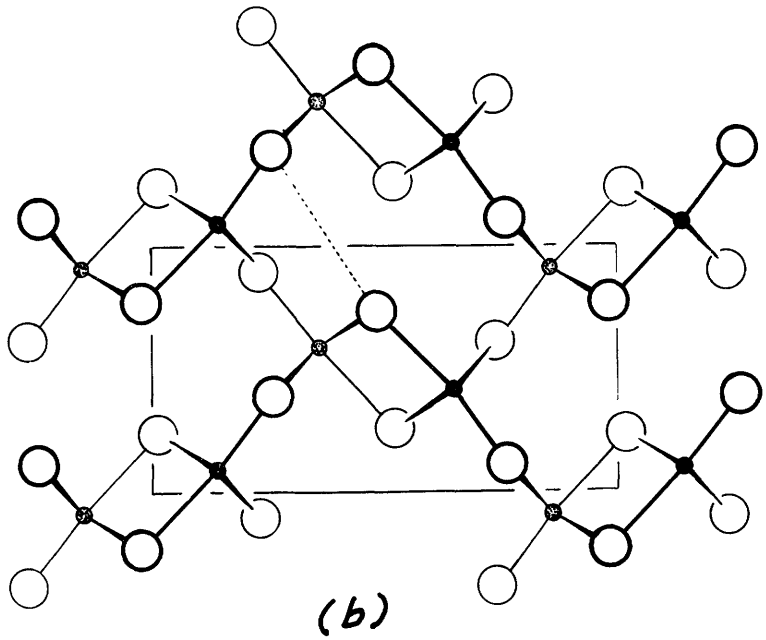

Figure 4.--View of crystal structures along the c axis of (a) montroseite and (b) paramontroseite.